ON THE NATURE OF THE FAINT COMPACT NARROW EMISSION-LINE GALAXIES: THE HALF-LIGHT RADIUS–VELOCITY WIDTH DIAGRAM[1]

RAFAEL GUZMÁN, DAVID C. KOO,[2] S. M. FABER, AND GARTH D. ILLINGWORTH

University of California Observatories/Lick Observatory, Board of Studies in Astronomy and Astrophysics, University of California, Santa Cruz, CA 95064

MARIANNE TAKAMIYA AND RICHARD G. KRON[2]

Department of Astronomy and Astrophysics, University of Chicago, 5460 South Ellis Avenue, Chicago, IL 60637

AND

MATTHEW A. BERSHADY[2, 3]

Department of Astronomy and Astrophysics, Pennsylvania State University, 525 Davey Lab, University Park, PA 16802

ABSTRACT

We present new measurements of emission-line velocity widths for five faint compact narrow emission-line galaxies (CNELGs) with $20.5 \leq B \leq 21.5$ and redshifts $z \sim 0.19$ to 0.35. The spectra were taken at the Keck telescope using the HIRES spectrograph with a resolution of 8 km s^{-1} (FWHM). Emission-line profiles are roughly Gaussian with velocity widths $\sigma \sim 30$ to 50 km s^{-1}. The new σ data, in combination with *Hubble Space Telescope* (*HST*) measurements of half-light radii R_e, indicate that these CNELGs are low-mass stellar systems (i.e., $M \sim 10^9 \, M_\odot$), while their unusually low mass-to-light ratios (typically $<0.2 \, M_\odot/L_\odot$) are consistent with being undergoing a major burst of star formation. Since R_e and σ are roughly independent of the fading of the stellar population, the R_e–σ diagram is particularly useful for comparing the properties of these young galaxies to those of evolved stellar systems. Several physical processes that may modify the position of CNELGs in this diagram during their evolution, including dissipation, mergers, stripping, and winds, are discussed briefly. We conclude that the new data support a simple evolutionary scenario in which these low-mass, young galaxies will fade after the starburst, without major changes in R_e or σ, to become today's spheroidal galaxies.

Subject headings: cosmology: observations — galaxies: compact — galaxies: evolution — galaxies: formation — galaxies: fundamental parameters

1. INTRODUCTION

The nature of the numerous faint blue galaxies observed in deep images of the sky is one of the major unresolved questions of modern cosmology (see review by Koo 1994 and references therein). The high surface density and weak clustering of these galaxies argue against their being either the progenitors or the merging components of present-day bright galaxies (Lilly, Cowie, & Gardner 1991; Efstathiou et al. 1991). Various theoretical scenarios have instead suggested that the faint blue galaxies are low-mass stellar systems experiencing their initial starburst at redshifts $z \leq 1$, some of which turn into the present population of spheroidal galaxies[4] (Babul & Rees 1992; Babul & Ferguson 1996).

A new approach to investigate the nature of these faint galaxies is to compare their global properties (i.e., sizes, surface brightnesses, luminosities, internal velocities, and abundances) to those of the local population. This Letter is part of a series of papers aimed at studying the properties of a subset of faint blue galaxies characterized by being very compact and having narrow emission lines (so-called

CNELGs; Koo et al. 1994, 1995). One of the main results of these studies is the identification of extreme star-forming systems like H II galaxies as the local counterparts of CNELGs. Using evolutionary stellar population models, Koo et al. (1995) have also shown that, without additional star formation, CNELGs will fade to match the low luminosities and surface brightnesses of the brightest nearby spheroidal galaxies. In this Letter, we show that CNELGs are indeed low-mass stellar systems using a unique data set that includes *Hubble Space Telescope* (*HST*) measurements of half-light radii (R_e) and Keck measurements of velocity widths (σ) for a sample of seven of these galaxies. We also show that their position in the R_e–σ diagram supports the idea that CNELGs may evolve into today's spheroidals.

2. NEW OBSERVATIONS

The seven galaxies in our sample are the brightest objects in a set of 35 CNELGs at $z \sim 0.1$–0.7 (Koo & Kron 1988; Munn et al. 1996). Ground-based measurements of magnitudes, colors, redshifts, and line-strength ratios, as well as *HST* measurements of effective radii and mean effective surface brightnesses, are given in Koo et al. (1994). Average values of these quantities for our CNELG sample are listed in Table 1. For two of these galaxies (i.e., Her 3618 and Her 13385), measurements of velocity widths derived from previous spectroscopic observations are given in Koo et al. (1995). Spectra of the remaining five objects were taken on 1994 October 2–4, using the high-resolution echelle spectrograph HIRES (Vogt et al. 1994) at the W. M. Keck 10 m telescope. The seeing was

---

[1] Based on observations obtained at the W. M. Keck Observatory, which is operated jointly by the University of California and the California Institute of Technology.

[2] Visiting Astronomer, Kitt Peak National Observatory (KPNO), National Optical Astronomy Observatories, which is operated by AURA under cooperative agreement with the National Science Foundation.

[3] Hubble Fellow.

[4] We adopt in this paper the nomenclature suggested by Kormendy & Bender (1994), i.e., low-density, dwarf ellipsoidal galaxies like NGC 205 are called "spheroidals" instead of "dwarf ellipticals."

TABLE 1
Average Observed Properties of CNELGs[a]

Parameter	z	R_e (kpc)	B (mag)	M_B (mag)	$(U-B)_0$ (mag)	$(B-V)_0$ (mag)	SB_e (mag arcsec^{-2})	[O III]/Hβ	[N II]/Hα	σ (km s^{-1})
Average	0.217 ± 0.034	1.40 ± 0.11	21.01 ± 0.09	-19.86 ± 0.43	-0.24 ± 0.04	0.39 ± 0.03	19.01 ± 0.30	2.35 ± 0.38	0.19 ± 0.03	45 ± 5
rms	0.090	0.29	0.24	1.14	0.11	0.08	0.79	1.00	0.08	13

[a] Rest-frame quantities [R_e, M_B, $(U-B)_0$ and $(B-V)_0$] assume $q_0 = 0.1$ and $H_0 = 50$ km s^{-1} Mpc^{-1}.

~0″.8 FWHM. The 1″.15 × 14″ slit yielded a FWHM spectral resolution of 8 km s^{-1} on the Tektronix 2048^2 CCD. All exposures were 1800 s, except for Lyn 2-11500, which was observed for 1500 s. Internal quartz lamp frames for flat fields and Th-Ar arc lamp frames for wavelength calibration were taken after observing each galaxy.

The spectra were reduced using standard techniques described in the IRAF/NOAO "echelle" package. After flat-fielding, cosmic-ray removal, correction for scattered light and sky-subtraction, the central 5 pixels (i.e., 1″) were co-added to produce one-dimensional spectra in velocity space. Four echelle orders spanning the rest wavelength region ~3700–5100 Å were typically used in the analysis. The signal-to-noise ratio of several emission lines is high enough to allow measurements of velocity widths (mainly the [O II] λ3727 doublet, Hβ, [O III] λ4059, and [O III] λ5007). To a good approximation, the line profiles are well fitted by Gaussians. Hence we characterize the width of the lines by the rms velocity dispersion (σ = FWHM/2.35). The final σ values listed in Table 2 are the unweighted average of fits to several lines. From the variance among different lines, we estimate that the uncertainty is ~6%. The average velocity width for our sample is $\langle\sigma\rangle = 45$ km s^{-1}.

In Figure 1 we show the data points for the [O III] λ5007 Å emission lines and the average Gaussian profiles. For completeness, we also show the same plots for Her 3618 and Her 13385 (from Koo et al. 1995). Although a Gaussian provides a reasonably good fit to the line profiles, there are some hints that the kinematics of the ionized gas may be more complex than just random motions. In particular, the [O III] lines of SA 68-17255 show extended wings compared to their Gaussian fits, while those of Lyn 2-11378 appear to be best fitted by two Gaussian profiles. The two components are separated by ~80 km s^{-1} in velocity space. Similar anomalies have been observed in some nearby low-mass stellar systems that are undergoing, or have recently experienced, a major starburst (Rosa & Solf 1984; Skillman & Balick 1984). In particular, Marlowe et al.

(1994) have shown that the emission-line profiles of the ionized gas in some dwarf amorphous galaxies are double or multiply peaked, and the kinematics are consistent with kiloparsec-scale structures expanding at typical velocities of 20–100 km s^{-1}. The observed expansion of the ionized interstellar medium is likely to be a transient event resulting from starburst-driven galactic winds. The effect of this physical process on the galaxy structure and kinematics is further discussed in § 4.

3. MASS ESTIMATES OF THE CNELGS

The observed properties of CNELGs, i.e., very blue colors, small sizes, high luminosities, strong emission lines, and low velocity widths (see Table 1), suggest that these distant objects most resemble the local population of low-mass, extreme star-forming H II galaxies (Koo et al. 1994, 1995). A new, fundamental dimension to understand the nature of CNELGs is their mass. Being independent of the luminosity evolution, mass allows a direct comparison with today's evolved stellar systems. The masses of CNELGs can be estimated via the virial theorem using the new R_e and σ data set listed in Table 2. However, a word of caution is needed when using half-light radii and emission-line velocity widths in star-forming galaxies to characterize the galaxy size and gravitational potential. For instance, if the star-forming event does not occur globally, then the half-light radius may underestimate the actual galaxy size. In addition, the velocity width may reflect turbulent motions of the ionized gas due to stellar winds instead of virialized motions due to gravity. Even if gravity dominates the gas kinematics, the emission-line velocity widths will depend on the space distribution of the ionized gas. Before determining the masses of CNELGs we briefly address these concerns.

Although CNELGs are clearly undergoing a major star-forming event, they may possess a very faint, underlying, extended old population. Indeed, deep CCD images of compact H II galaxies have revealed the existence of such an extended older stellar component (Telles 1995). For a sample of H II galaxies with similar luminosities and velocity widths to our CNELG sample (data from Telles 1995), we estimate that the half-light radius of the underlying population is, on average, twice the characteristic size of the starburst region. This suggests that, if CNELGs have a similar older stellar component, their characteristic sizes may be underestimated by a factor ~2. Deep near-infrared observations are needed, however, to check for the real extent of any underlying population in distant CNELGs.

Perhaps more important for mass determinations is the issue of the relation between the observed velocity widths and the galaxy gravitational potential. For H II galaxies, this subject has been discussed by Terlevich & Melnick (1981). The similarity of the L–σ and R_e–σ correlations with those of self-gravitating systems led them to favor gravity as the mechanism that dominates the gas kinematics. This interpre-

TABLE 2
Masses and Mass-to-Light Ratios of CNELGs

ID	R_e (kpc)	σ (km s^{-1})	M[a] (10^9 M$_\odot$)	$(M/L_B)_e$ $(M/L)_\odot$
Lyn 2-11378........	1.60	49	4.55	0.07
Lyn 2-8115..........	1.44	53	4.80	0.17
Lyn 2-11500........	1.72	29	1.72	0.07
Her 13385..........	0.94	68	5.15	0.87
Her 3618............	1.15	28	1.07	0.09
SA 68-17255	1.70	40	3.22	0.02
SA 68-6134	1.29	41	2.57	0.05

[a] Masses were determined from $M = 3 kG^{-1} R_e\sigma^2$, where the structural constant k varies with different galaxy surface density profiles. Since the surface brightness profile of CNELGs is consistent with an exponential law (Koo et al. 1994), we adopt $k \sim 1.6$ (Bender, Burstein, & Faber 1992).
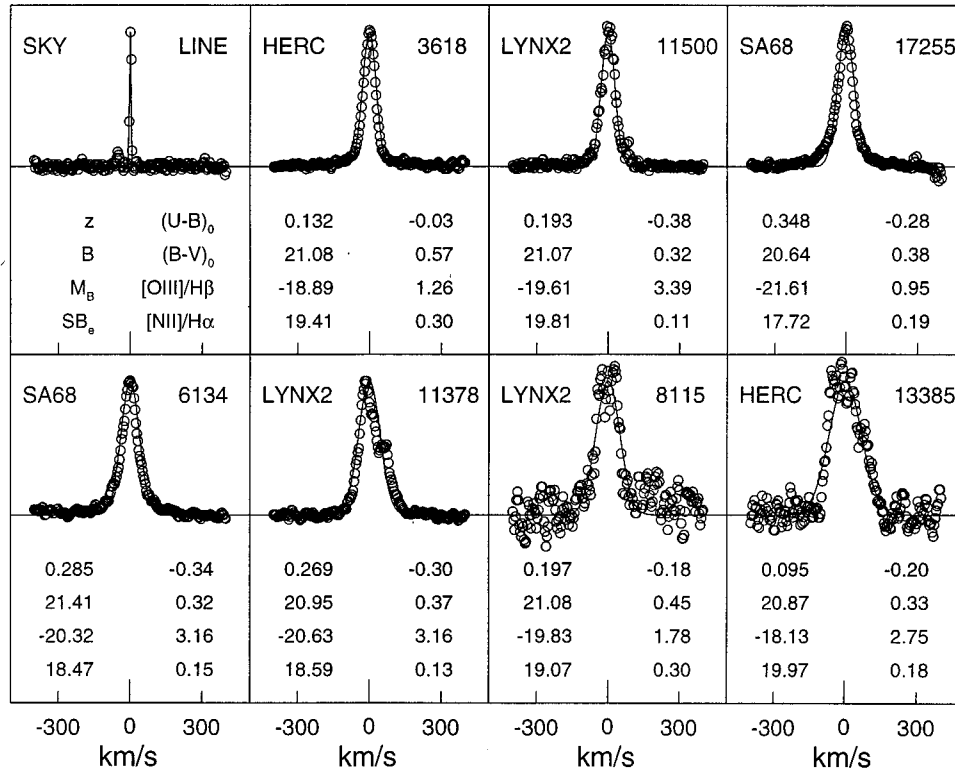
Fig. 1.—Panel of new [O III] $\lambda5007$ emission-line profiles in km s^{-1} for five CNELGs. For completeness, we also show the emission-line profiles of Her 13385 and Her 3618 (Koo et al. 1995). In the upper left panel, a typical night sky line shows our instrumental resolution of $\sigma = 3.4$ km s^{-1}. Each panel is labeled at the top with the ID name (field and number) and includes the redshift (z), apparent blue B_J magnitude, rest-frame B absolute magnitude (M_B), rest-frame B surface brightness in mag arcsec^{-2} (SB_e), rest-frame $U - B$ and $B - V$ colors, and [O III $\lambda5007$]/Hβ and [N II $\lambda6583$]/Hα line ratios, in positions as shown in the upper left panel. Solid lines show the best Gaussian curve that fits the average of profiles from all emission lines. Note the presence of a second component in Lyn 2-11378 and the extended wings in SA 68-17255.

tation is supported by recent models of star-forming regions showing that, just after formation, stellar winds of low-mass stars moving with a velocity dispersion σ_* will stir the remaining gas cloud, providing it with an average turbulent motion $\sigma \sim \sigma_*$ (Tenorio-Tagle, Muñoz-Tuñón, & Cox, 1993). Comparison between the 21 cm and [O III] line widths further strengthens this conclusion. For a sample of 11 H II galaxies and H II regions listed in Telles & Terlevich (1992), we derive $\langle \sigma([\mathrm{O\ III}])/\sigma(21\ \mathrm{cm}) \rangle = 0.7 \pm 0.1$. Independently of the physical mechanism responsible for the motions of the ionized gas, this comparison suggests that the [O III] line widths can be used to estimate the galaxy gravitational potential. The observed 30% difference may simply reflect the different spatial scales of the ionized and neutral gas, since the space distribution of [O III] is typically more compact than the extended H I cloud (Taylor et al. 1995). Since CNELGs are similar to H II galaxies, the measured velocity widths are likely to underestimate their internal velocities by as much as $\sim$30%.

In Table 2 we list the virial masses for our CNELG sample. Note that these estimates are not total masses but are representative of the matter within R_e and can be directly compared to similar mass estimates for the various galaxy types at the current epoch. The values listed in Table 2 range from $\sim$1 to 5×10^9 $M_\odot$. Although, according to the discussion above, these masses may be underestimated by as much as a factor $\sim$4, they are much smaller than the characteristic masses of giant stellar systems such as normal elliptical or spiral galaxies (typically $\sim$$10^{11}$ $M_\odot$). We therefore conclude that CNELGs are indeed low-mass stellar systems. Finally, in Table 2 we also

list the derived mass-to-light ratios within R_e. Six of the seven CNELGs have $(M/L)_e$ values ranging from 0.02 to 0.17, in solar units. Even after a factor 4 increase in mass, these very low values suggest that CNELGs are undergoing a major starburst with a current star formation rate that may be as much as $\sim$10 times higher than their average star formation rate (Kennicutt, Tamblyn, & Congdon 1994).

4. HALF-LIGHT RADIUS–VELOCITY WIDTH DIAGRAM

The R_e–σ diagram is particularly useful to study how distant young galaxies relate to nearby evolved stellar systems, since the position of galaxies in this diagram is not strongly dependent on the amount of fading experienced by their stellar populations. In Figure 2 we show the R_e–σ diagram for our CNELG sample as well as for a representative sample of various types of nearby galaxies. Low-density galaxies (spheroidals and irregulars) and low-mass star-forming systems (H II and dwarf amorphous) are clearly segregated from ellipticals and spirals. CNELGs lie on top of the distribution of low-density galaxies and star-forming systems.[5]

---

[5] The following points are relevant for an adequate interpretation of Figure 2: (1) The observed galaxy distribution does not vary significantly if larger galaxy samples are included. The R_e–σ diagram for $\sim$1000 nearby galaxies shows a similar galaxy distribution (data from D. Burstein, private communication). (2) The relative position of the various galaxy types is not greatly affected by minor corrections for inclination or aperture effects to the "raw" σ values used in this figure. Velocity widths are defined as FWHM/2.35 for all galaxy types, independently of the shape of the line profile, whether they are measured from stellar absorption features or gas emission lines and whether
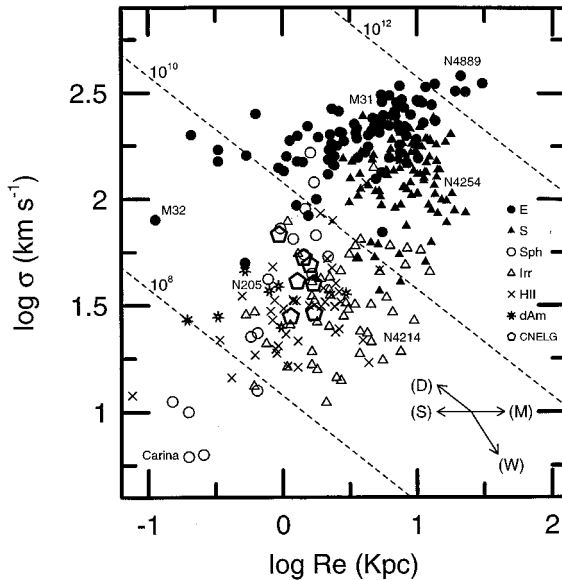
FIG. 2.—The half-light radius (R_e) vs. velocity width (σ) diagram for various galaxy types: *open pentagons*, CNELGs (this paper); *filled circles*, E/S0 galaxies (Bender et al. 1992); *filled triangles*, spirals (de Vaucouleurs et al. 1991); *open triangles*, irregulars (de Vaucouleurs et al. 1991); *open circles*, spheroidals (Bender et al. 1992); *crosses*, H II galaxies (Telles 1995) and *stars*, dwarf amorphous galaxies (Marlowe et al. 1994). For convenience, a few galaxies representative of today's evolved stellar systems have been identified. The arrows represent the direction in which R_e and σ change due to different physical processes as explained in the text: (*D*) dissipation; (*M*) mergers; (*S*) tidal stripping; (*W*) galactic winds. The dashed lines correspond to constant-mass lines of 10^8, 10^{10}, and 10^{12} solar masses, respectively. Along these lines, mass surface-density decreases uniformly from the upper left to the bottom right part of the diagram.

The position of CNELGs on the R_e–σ diagram suggests that these galaxies are related, both structurally and kinematically, to the nearby population of spheroidal and irregular galaxies. There are, however, several physical processes that may alter both R_e and σ during galaxy evolution. Following Bender, Burstein, & Faber (1992), we sketch various possible "evolutionary paths" for CNELGs on the R_e–σ diagram associated with the most important processes:

1. *Dissipation.*—Energy dissipation will enhance the density of the baryonic component, increasing σ while conserving the mass. Hence, dissipation is likely to move CNELGs toward larger values of σ and smaller values of R_e such that $R_e\sigma^2 \sim$ constant. The "dissipation" vector (*D*) roughly points toward the location of M32-type elliptical galaxies.

2. *Mergers.*—Mergers between galaxies or among their progenitors most likely occur in a hierarchical manner. Numerical simulations show that the structure of the merger remnants is such that R_e increases after each merger while σ remains

unchanged (Hernquist, Spergel, & Heyl 1993). The "merging" vector (*M*) is thus parallel to the R_e axis and points toward the location of low-mass spirals and irregular galaxies.

3. *Tidal stripping.*—To a first approximation, stripping of stars from the outer parts of a galaxy will leave σ approximately constant and reduce R_e (Nieto & Prugniel 1987). Using Aguilar & White's (1985) models, we estimate that typical tidal interactions between galaxies in low-density environments may change R_e by only a few percent. Hence, the "tidal stripping" vector (*S*) will move CNELGs toward smaller R_e, but the effect is very small.

4. *Galactic winds.*—Gas removal due to starburst-driven galactic winds is likely to be one of the most important processes that determine the final structure and stellar content of low-mass galaxies (Larson 1974; Yoshii & Arimoto 1987; Dekel & Silk 1987). Adiabatic mass loss will make the galaxy expand while keeping the product $R_e\,\sigma \sim$ constant (Vader 1986). The expected change in R_e and σ for a spherical galaxy with $M \sim 10^9$–10^{10} $M_\odot$ is $\Delta \log R_e = -\Delta \log \sigma \sim 0.3$ dex (Yoshii & Arimoto 1987), although the effect may be significantly smaller depending on the geometry and multiphase nature of the interstellar medium (de Young & Heckman 1994) or the extent of any dark matter halo. The "galactic wind" vector (*W*) points downward toward the location of the lower density irregular galaxies.

5. *Ram pressure stripping.*—This process affects mainly galaxies within the hot intergalactic medium of galaxy clusters, and the effect is similar to the galactic winds. Since CNELGs are located in low-density environments, this process is probably negligible.

The discussion above provides interesting consequences for the evolution of our CNELGs. First, although energy dissipation may, in principle, transform CNELGs into low-mass ellipticals, the large amount of dissipation required to increase σ by a factor ~ 3 while reducing R_e by one order of magnitude makes this possibility very unlikely. Second, CNELGs cannot become low-mass spiral galaxies as a result of mergers, since the merging process will destroy the disks and leave the remnants with a spheroidal-like structure (Quinn 1982). Third, galactic winds may plausibly transform CNELGs into lower density irregular or spheroidal galaxies. The evolution of CNELGs into one galaxy class or another may depend critically on their ability to retain part of their interstellar medium after the winds. Their extremely low mass-to-light ratios suggest that the kinetic energy supplied by the current starburst in CNELGs is likely to be large enough, compared to their binding energy, to blow out most of the gas, halting thus the star-forming process. Without additional star formation, Koo et al. (1995) have shown that CNELGs will fade to resemble today's spheroidals. There are also other arguments in favor of this evolutionary scenario as opposed to CNELGs evolving into irregulars. In particular, the average metallicity of our CNELG sample (~ 0.7 solar) is similar to that of spheroidals with similar velocity widths (Peterson & Caldwell 1993), but larger than that of irregular galaxies (typically ~ 0.5 solar; Hunter & Gallagher 1986). More compelling is the lack of evidence for a CNELG phase, i.e., a dominant early burst, in the star formation history of nearby irregulars (Skillman & Bender 1995). The nearly constant star formation rate of these galaxies poses a serious challenge to the idea that CNELGs may be the progenitors of irregular galaxies. Alternatively, all

---

they are global or central values. Corrections for such effects will change slightly the relative position of galaxies in this diagram. The largest shift relative to the position of CNELGs applies to spiral galaxies. This is in the sense that the equivalent σ values for spirals would be, on average, ~ 0.15 dex smaller. (3) Samples of spheroidal galaxies with σ measurements in the literature are strongly biased toward high surface brightness objects. Using the framework of galaxy properties described in Guzmán et al. (1993) and the average $M_B - SB_e$ relation for a complete sample of Virgo spheroidals (Binggeli & Cameron 1991), we estimate that, compared to our sample, the "average" spheroidal galaxy will have lower σ by ~ 0.2 dex at a given R_e.

well-observed spheroidals appear to have experienced a dominant burst of star formation only several billion years ago (Skillman & Bender 1995). If we could trace back in time the star formation history of spheroidal galaxies, what would these dominant bursts look like? The answer is simple: they would have luminosities, surface brightnesses, colors, and redshifts virtually identical to those actually observed in our CNELGs (Koo et al. 1995). The simplest interpretation of the $R_e-\sigma$ diagram thus strengthens the conclusion that a class of galaxies at intermediate redshifts, the CNELGs, has been identified as being among the progenitors of today's spheroidal galaxies.

REFERENCES

Aguilar, L., & White, S. D. M. 1985, ApJ, 295, 373
Babul, A., & Ferguson, H. C. 1996, ApJ, 458, 100
Babul, A., & Rees, M. J. 1992, MNRAS, 255, 346
Bender, R., Burstein, D., & Faber, S. M. 1992, ApJ, 399, 462
Binggeli, B., & Cameron, L. M. 1991, A&A, 252, 27
Dekel, A., & Silk, J. 1986, ApJ, 303, 39
de Vaucouleurs, G., de Vaucouleurs, A., Corwin, H. G., Buta, R. J., Paturel, G., & Fouqué, P. 1991, Third Reference Catalog of Bright Galaxies (New York: Springer) (RC3)
De Young, D., & Heckman, T. M. 1994, ApJ, 431, 538
Efstathiou, G., Berstein, G., Katz, N., Tyson, J. A., & Guhatakurta, P. 1991, ApJ, 380, L47
Guzmán, R., Lucey, J. R., & Bower, R. G. 1993, MNRAS, 265, 731
Hernquist, L., Spergel, D. N., & Heyl, J. S. 1993, ApJ, 416, 415
Hunter, D. A., & Gallagher, J. S. 1986, PASP, 98, 5
Kennicutt, R. C., Tamblyn, P., & Congdon, C. W. 1994, ApJ, 435, 22
Koo, D. C. 1994, in IAU Symp. 168, Examining the Big Bang and Diffuse Background Radiations, ed. M. Kafatos (Dordrecht: Kluwer), in press
Koo, D. C., Bershady, M. A., Wirth, G. D., Stanford, S. A., & Majewski, S. R. 1994, ApJ, 427, L9
Koo, D. C., Guzmán, R., Faber, S. M., Illingworth, G. D., Bershady, M. A., Kron, R. G., & Takamiya, M. 1995, ApJ, 440, L49
Koo, D. C., & Kron, R. G. 1988, ApJ, 325, 92
Kormendy, J., & Bender, R. 1994, in Proc. ESO/OHP Workshop on Dwarf Galaxies, ed. G. Meylan & P. Prugniel (Garching: ESO), 161
Larson, R. B. 1974, MNRAS, 169, 229
Lilly, S. J., Cowie, L. L., & Gardner, J. P. 1991, ApJ, 369, 79
Marlowe, A. T., Heckman, T. M., Wyse, R. F. G., & Schommer, R. 1995, ApJ, 438, 563
Munn, J. A., Koo, D. C., Kron, R. G., Majewski, S. R., Bershady, M. A., & Smetanka, J. J. 1996, ApJS, submitted
Nieto, J. L., & Prugniel, P. 1987, in IAU Symp. 127, Structure and Dynamics of Elliptical Galaxies, ed. T. de Zeeuw (Dordrecht: Reidel), 99
Peterson, R. C., & Caldwell, N. 1993, AJ, 105, 1411
Quinn, P. 1982, Ph.D. thesis, Australian National Univ.
Rosa, M., & Solf, J. 1984, A&A, 130, 29
Skillman, E. D., & Balick, B. 1984, ApJ, 280, 380
Skillman, E. D., & Bender, R. 1995, in Proc. 5th Texas-Mexico Conf. on Astrophysics, in press
Taylor, C. L., Brinks, E., Grashuis, R. M., & Skillman, E. D. 1995, ApJS, 99, 448
Telles, E. 1995, Ph.D. thesis, Univ. of Cambridge
Telles, E., & Terlevich, R. 1993, Ap&SS, 205, 49
Tenorio-Tagle, G., Muñoz-Tuñón, C., & Cox, D. P. 1993, ApJ, 418, 767
Terlevich, R., & Melnick, J. 1981, MNRAS, 195, 839
Vader, J. P. 1986, ApJ, 305, 669
Vogt, S., et al. 1994, Proc. SPIE, 2198, 362
Yoshii, Y., & Arimoto, N. 1987, A&A, 188, 13